IEEE Access
Multidisciplinary | Rapid Review | Open Access Journal

Received September 4, 2019, accepted October 2, 2019, date of publication October 9, 2019, date of current version October 24, 2019.

Digital Object Identifier 10.1109/ACCESS.2019.2946388

On-Field *In situ* Inspection for *Marssonina Coronaria* Infected Apple Blotch Based on Non-Invasive Bio-Photonic Imaging Module

JUNSOO LEE[1], SEUNG-YEOL LEE[2], RUCHIRE ERANGA WIJESINGHE[3], NARESH KUMAR RAVICHANDRAN[1], SANGYEOB HAN[1], PILUN KIM[4], MANSIK JEON[1], HEE-YOUNG JUNG[2], AND JEEHYUN KIM[1], (Member, IEEE)

[1]School of Electronics Engineering, College of IT Engineering, Kyungpook National University, Daegu 41566, South Korea
[2]School of Applied Biosciences, Kyungpook National University, Daegu 41566, South Korea
[3]Department of Biomedical Engineering, Kyungil University, Gyeongsan 38428, South Korea
[4]School of Medicine, Kyungpook National University, Daegu 41566, South Korea

Corresponding authors: Hee-Young Jung (heeyoung@knu.ac.kr) and Jeehyun Kim (jeehk@knu.ac.kr)

This work was supported in part by the Bio and Medical Technology Development Program of the National Research Foundation (NRF) through the Korean Government under Grant 2017M3A9E2065282, in part by the National Research Foundation of Korea (NRF) through the Korean Government under Grant 2018R1A5A1025137, in part by the Basic Science Research Program under the National Research Foundation of Korea (NRF) through the Ministry of Education under Grant 2018R1D1A1B07043340, and in part by the BK21 Plus Project through the Ministry of Education, South Korea, under Grant 21A20131600011.

ABSTRACT On-field *in situ* inspection of *Marssonina coronaria* infected apple blotch for apple leaf specimens was demonstrated using compact backpack-type optical coherence tomography (OCT). Simultaneously, the acquired OCT results were precisely matched with a widely used agricultural plant pathogen inspection technique called loop-mediated isothermal amplification (LAMP) to confirm on-field applicability of the compact backpack-type OCT. Specimens were examined for 8 weeks. Automated Amplitude-scan (A-scan) depth profiling and post-processed infected tissue boundary detection from acquired OCT images were performed to investigate the increase in the internal layer gaps of the leaf specimens resulting from the disease. Clearly identifiable morphological difference between healthy and infected-suspected specimens was observed through the OCT images, which were well correlated with LAMP results. OCT-LAMP correlations and confirmed feasibility study results conclude that the compact backpack-type OCT diagnosing modality can be effective and extensively applicable for various novel agricultural discoveries.

INDEX TERMS Optical coherence tomography, loop-mediated isothermal amplification, apple blotch, *Marssonina coronaria*, optical inspection.

I. INTRODUCTION

Apple blotch caused by *Marssonina coronaria* is one of the worst fungal diseases occurs in apple cultivation [1]. Apple blotch was first reported in Japan and now it is a common apple disease not only in Asia, but also in North America, and Oceana. In general, diseased apple trees results in leaf discoloration and finally defoliated. In Korea, it was reported that conidia of *M. coronaria* spreads between May and June, which has a long incubation period of 2-6 weeks compared to other fungal disease [2]. Thus, the disease can only be controlled once the symptoms are externally appeared. Due to this difficulty, most of farmers use the fungicide spraying technique, which can result in overuse [1]. Furthermore, leaf defoliation during the growing season results quality and yield loss of the fruit [3]. Therefore, according to the agricultural point of view, early diagnosis can be the prominent solution to control the apple blotch.

Nucleic acid amplification with polymerase chain reaction (PCR) have been widely used in plant pathology to diagnose infectious diseases [5, 6]. However, there are major disadvantages, such as necessity of a precision instrument for amplification, elaborate method for detection of the amplified products, and destructiveness [6]. Furthermore, the applicability of the methods in agriculture orchards is limited due to system complexity and high time consumption.

The associate editor coordinating the review of this manuscript and approving it for publication was Abdel-Hamid Soliman.

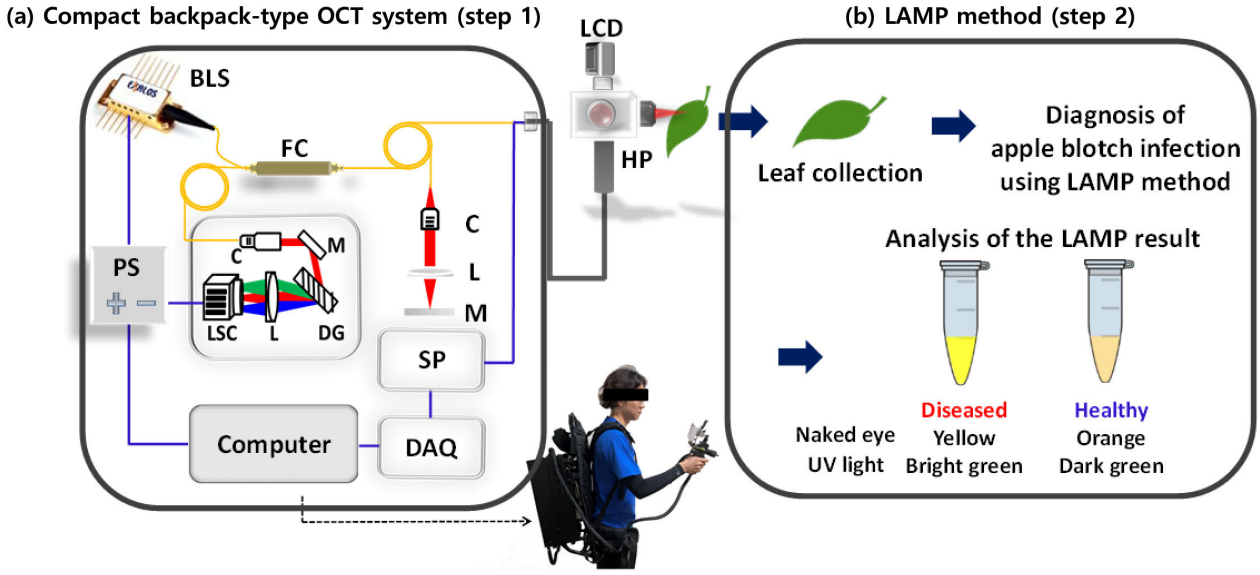

FIGURE 1. Schematic diagram of (a) the compact backpack-type OCT system along with (b) the LAMP methodology. Inspection using LAMP technique (Step 2) was performed after OCT imaging (Step 1). BLS: broadband laser source, C: collimator, DG: diffraction grating, FC: fiber coupler (50 × 50), HP: handheld probe, L: lens, LSC: line scan camera, M: mirror, PS: power supply, SP: signal processing.

Loop-mediated isothermal amplification (LAMP) technique is an isothermal nucleic acid amplification technique, which is conducted at a constant temperature of 60°C to 65°C, and does not require a thermal cycler, while PCR technology needs an alternating temperature steps or cycles [7], [8]. LAMP can efficiently amplify a few copies of DNA in a short time and provide high specificity for the target sequence. In addition, once the appropriate primers are prepared, this simple agricultural inspection technique can be performed easily [9], [10].

Besides these numerous agricultural inspection techniques, morphological and structural imaging of the plant materials has been attempted non-invasively to circumvent specimen destructive issues using X-rays [11], magnetic resonance imaging (MRI) [12], positron emission tomography (PET) [13] and ultrasound imaging [14]. However, shortcomings of low resolution and long acquisition time barricade the applicability of these methods for precise analysis. In order to overcome the aforementioned major limitations of the imaging modalities, non-destructive high-resolution optical imaging techniques have gained plenty of interest recently.

Among high-resolution optical inspection modalities, optical coherence tomography (OCT) is a well-known non-destructive imaging technology that provides cross-sectional images of various biological tissue specimens with a micrometer range resolution. Since OCT is capable of providing real-time images with an exceptional resolution, OCT has been involved extensively in variety of medical applications including ophthalmology [15], [16], dentistry [17], [18], and dermatology [19], [21]. The scan depth of OCT is suitable for examining the internal structure of plant leaves, since it provides a higher scan depth with a microscopic resolution similar to a conventional microscope [22], [23]. In addition, previously demonstrated OCT based agricultural disease and material inspection studies provided a solid platform confirming the applicability of OCT for plant material inspection [24]–[32].

The main purpose of the proposed study was to demonstrate on-field *in situ* inspection for apple leaf specimen to diagnose apple blotch using the laboratory developed compact backpack-type OCT system. An agricultural inspection method, called LAMP technique, was simultaneously performed to confirm the correlation between LAMP and OCT results, which were acquired using the developed inspection modality. Therefore, our study highlights the on-field *in situ*inspection for apple blotch using our own developed OCT with the verification by LAMP technique and the incorporation of both OCT and LAMP techniques as an inspection protocol for the pre-identification of apple blotch. In addition to the high-resolution OCT cross-sectional images, automated Amplitude-scan (A-scan) depth profiles provided a verification of the morphological state (as healthy or infected) emphasizing the effectiveness of proposed method as a promising diagnostic approach in agriculture.

II. MATERIALS AND METHODS

A. COMPACT BACKPACK-TYPE OCT SYSTEM

The developed compact backpack-type OCT system shown in Fig. 1(a) (Step 1) contains a customized spectrometer and power battery along with a broadband light source of superluminescent diode (EXS210068-01, Exalos, Switzerland) with a center wavelength of 850 nm and a bandwidth of 55 nm. In the spectrometer, a 2048-pixel line scan camera (spL2048-140km, Basler, Germany) was used as the optical detector, and the components were precisely calibrated to

enhance the axial resolution and signal-to-noise ratio (SNR) of the system according to a method reported in [33]–[35]. All the hardware components were controlled by software algorithm written in C++ and LabVIEW. Sample scanning method includes a hand-held probe-based sample arm equipped with a galvanometer-based optical scanner (GVS002, Thorlabs, USA) for transverse scanning and a LCD screen for displaying 2D OCT image in real-time. The axial resolution of the system was 8 μm and the lateral resolution of 12 μm in the air.

For the mechanical structure of the compact backpack-type OCT system, a customized spectrometer and reference arm were designed and constructed to accommodate the optical system. Compared to previously developed agricultural inspection OCT modality [28], the dimensions of the spectrometer as well as reference arm were reduced, and all the components were made of aluminum with a total weight of 8 Kg. To control hardware devices, such as line scan camera and galvanometer scanners, a computer with an i3-4010U processor (NUC kit D34010WYKH, Intel, USA), a camera link frame grabber (PIXCI EB1mini, EPIX, USA), and a mini USB-based data acquisition (DAQ) board (NI USB-6212, NI) were used. A variable lens mount was designed to match the exact focus position, and the optical components of the handheld scanner probe were assembled into plastic case connected with 1.5 m long probe. LCD panel was attached to the handheld scanner with push buttons for viewing, capturing, and saving the OCT images in real-time. In addition, to increase the portability of the system and ensure continuous power consumption, a rechargeable power supply with an input voltage of 5 V was customized to provide an output voltage of 12-19 V.

Fig. 2 illustrates representative real-time information shown on the LCD screen, which is mounted on the handheld probe. The cross-sectional information of the specimen is displayed on top left corner along with the A-scan depth profile on top right corner. The raw fringe signal is presented underneath the 2D-OCT image. The red color dashed box with the word 'n = 200' indicated on 2D-OCT image emphasizes the region of interest of the A-scan profile acquired using total number of 200 A-lines. The unflatten biological nature of leaf specimens limits the capability of analyzing A-lines of the entire cross-section, where 200 A-lines were employed to ensure that the region of interest is included. The L1∼L3 shown on LCD describes the intensity peak information directly correlates to the specimen subsurface information, which was processed according to the refractive index of the material.

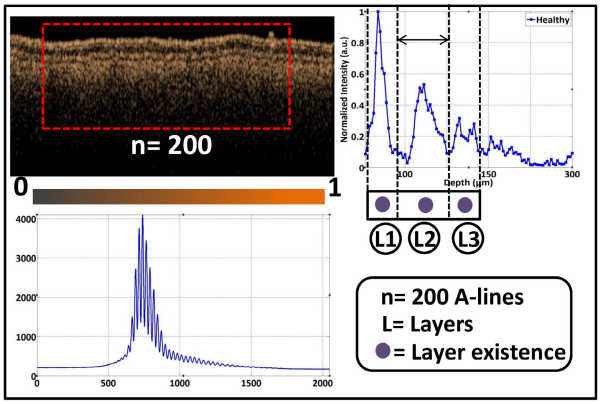

FIGURE 2. Elements shown on the LCD screen mounted on the handheld probe. OCT image, A-scan depth profile and raw fringe signal information are displayed all together in real-time.

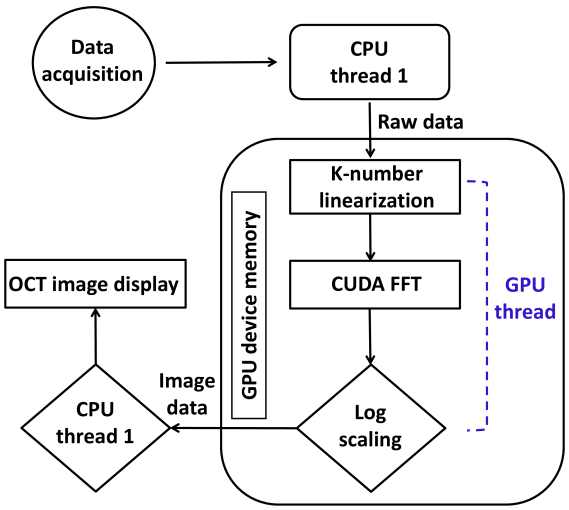

FIGURE 3. The flow chart of GPU accelerated signal processing architecture of the compact backpack-type OCT system.

B. SOFTWARE SETUP FOR FAST DATA PROCESSING

The software used for data acquisition, processing, and display was developed in LabVIEW and applied to the developed compact backpack-type OCT system. A compute unified device architecture (CUDA) with graphics processing units (GPU) was employed to enable fast data processing of raw OCT images. Fig. 3 shows the flow chart of programming architecture of compact backpack-type OCT system. The steps include the data flow between the CPU and the GPU, threads, and processing. The signal processing is divided into CUDA sub-processors to process the signal for OCT. Data processing includes wavenumber-number linearization, and fast Fourier transform. Full-range wavenumber-number linearization is used to eliminate the non-linearity of the raw signal [33], [34]. After log scaling, the processed data is sent back to the CPU thread, which displays the reconstructed OCT Brightness-scan (B-scan) image in real-time.

C. PLANT MATERIALS

Two apple orchards located in Sangju and Daegu in Gyeongbuk province, Korea were selected for the experiment. The selected apple orchards with annual yield are treated with fungicides and insecticide during cultivation. The regional statistical references were involved to select the orchards for

the on-field experiments, where the preference was given to the orchards. According to the annual reports, the incidence rate of apple blotch in Sangju orchard (cv. *Hongro*) was higher than the incidence rate of Daegu orchard (cv. *Fuji*). During the entire experimental process, the number of collected specimens per trial was 9 and 15 from Sangju and Daegu orchards, respectively. All leaf specimens were randomly collected. The entire experiment was carried out during early April to late May, while examining a total 144 leaf specimens at 6 experimental attempts.

D. LAMP TECHNIQUE

The leaf specimens, which were inspected using OCT, were collected and diagnosed for apple blotch infection using LAMP method (Fig. 1(b)). During LAMP reaction, the collected leaf surface was swiped using 70% ethanol, and each leaf specimen was ground. Sterilized leaves were extracted using a meshed sample bag (Agdia, Elkhart, IN) and tissue homogenizer (ACC00900, Agdia) in extraction buffer. Then, 1 μL of extraction buffer was added to a LAMP mixture (containing 10 $\times$ *Bst* reaction buffer, 10 mM dNTP, *M. coronariae* specific outer primer pair; Mar-F3 / Mar-B3 and inner primer pair Mar-FIP/Mar-BIP). Afterwards, the mixture was incubated at the optimized temperature using a digital water bath (JSWB-22T, JSR, Korea) for 5 min. Next, 1 μL of *Bst* polymerase large fragment (8 unit/μL, New England Biolabs, USA) was added, and the samples were incubated at the optimized for 1 hour. Finally, infection specimens were identified following the addition of 1 μL of SYBR green I®solution. After addition of SYBR green I®solution, bright green in UV illuminator (yellow to green in naked eye) was observed confirming the apple blotch infection, while dark green in UV illuminator (orange in naked eye) color illumination was observed through the healthy leaf specimens.

III. RESULTS AND DISCUSSION

While performing OCT examination, six specific locations were determined for all leaf specimens to acquire 2D-OCT images to ensure the consistency of the screening for various leaf specimens. All 2D-OCT images were scanned with a cross-sectional scanning range of 2 mm. The morphological behavior and functional changes occurred during the entire period of experiment are illustrated through the representative 2D-OCT images in Fig. 4. Fig. 4(a, c) show the representative 2D-OCT images acquired from Daegu plantation, and Fig. 4(b, d) from Sangju plantation. The leaf specimens, which were in a healthy state, provide a clear visualization of epidermal cell layer, palisade parenchyma, and spongy parenchyma without any abnormalities as shown in Fig. 4(a, b). However, a noticeable expansion of the gap between aforementioned leaf layers were identified in Fig. 4(c, d) signifying an infected state morphologically. The green dashed box regions indicated on Fig. 4(a, b) emphasize the healthy state, while red dashed box regions in Fig. 4(c, d) emphasize the infection revealing a large gap formation between layers as well as gradually faded epidermal cell layer. Since the

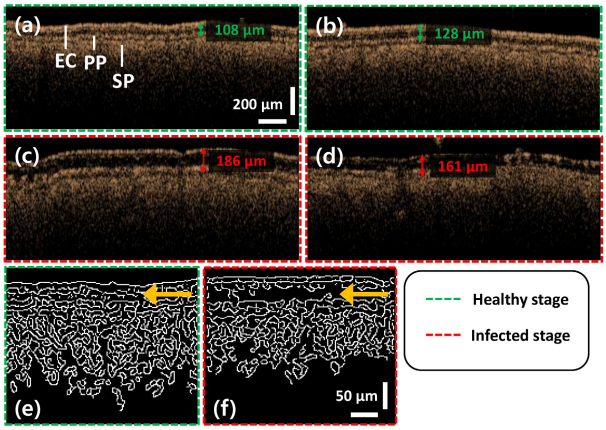

FIGURE 4. Representative 2D-OCT images according to a health state of the leaf specimens from each plantations. (a) and (c) are 2D-OCT images of the specimens in the Daegu plantation. (b) and (d) are 2D-OCT images of the specimens in the Sangju plantation. The distance between EC and PP layer is presented in each 2D-OCT images. (e) and (f) are Canny boundary detection images for (a) and (c), respectively. The color of dashed box represents a health state of each specimens. Yellow arrows in (e) and (f) indicate a notable change in the internal layers. EC: epidermal cell layer, PP: palisade parenchyma, SP: spongy parenchyma.

primary goal was to demonstrate on-field *in situ* inspection for apple blotch using backpack-type OCT system and obtain a simultaneous confirmation through LAMP technique, numerical representation regarding thickness expansion is illustrated in Fig. 4. The distance between epidermal cell layer and palisade parenchyma is increased from 108 μm to 186 μm in the specimen from Daegu plantation, and increased from 128 μm to 161 μm in the specimen from Sangju plantation. The threshold values for the intensity and the distance between the peaks were specified by the physical structure change of the specimen obtained through our previous experiments [25-30]. The quality of the OCT images were slightly degraded compared to commercial and laboratory based bench-top OCT systems due to the slight polarization mismatches, which were occurred during backpack-type system movements. However, the fundamental scope of the study was to confirm the on-field applicability for the real-time classification of infected leaf specimens. Since the expected internal gap expansion of layers and intensity differences were precisely visualized with a sufficient resolution, the acquired non-post processed raw OCT images were directly implemented to confirm the desired results. For detailed inspection, the structural gap formation and morphological abnormalities were further examined by considering the boundary information of the subsurface tissue regions using Canny boundary detection technique (shown in Fig. 4(e, f)) for the 2D-OCT images of Fig. 4(a, c) using a method reported in [35]. The obtained boundary detection results of leaf layer clearly reveal the morphological differences between healthy and infected stages.

As follows from the qualitative examination of the leaf specimens, acquired 2D-OCT images were involved to analyze depth dependent intensity information. Fig. 5 shows

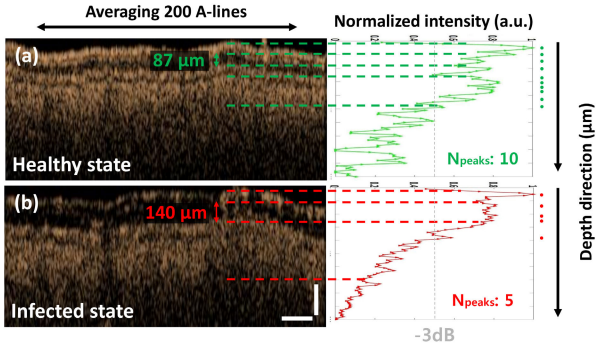

FIGURE 5. OCT cross-sectional images of leaf specimens in different health state along with the corresponding A-scan depth profiles. The number of peaks above -3 dB point in each A-scan depth profile is presented as the dots. (a) Healthy state, (b) infected state. The scale bars: 200 μm.

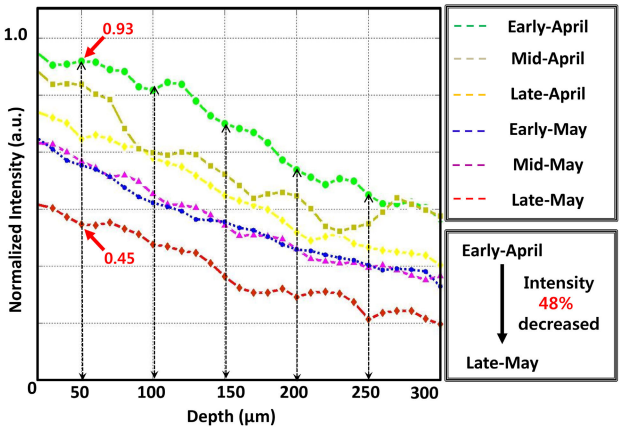

FIGURE 6. The representative averaged depth dependent normalized total intensity fluctuations correspond to each experimental period initiating from early-April to late-May. The intensity from 50 μm depth is decreased as 48% from the first experiment day (Early-April) to the last experiment day (Late-May).

the representative cross-sectional OCT images of inspected leaf specimens emphasizing healthy and infected states along with the corresponding A-scan depth profiles. The corresponding A-scan depth profile graphs are illustrated in green and red colors, respectively. The A-scan depth profile was obtained by averaging 200 A-lines from one 2D-OCT image and normalized by dividing the A-scan signal intensities into the maximum value. The state of internal leaf layers was clearly observed through A-scan depth profile information, such as the number of peaks and the spacing between intensity peaks. The intensity peak information of A-scan depth profile corresponding to the healthy specimen (Fig. 5(a)) reveals distinguishable individual layer information inside the leaf, while the noticeable disappearance of intensity peaks is revealed in the infected specimen (Fig. 5(b)). The number of peaks above -3 dB point is 10 for the healthy specimen and 5 for the infected specimen, which is 50% decrease as the infection is progressed. The gap between epidermal cell layer and palisade parenchyma is also increased approximately 60% from 87 μm to 140 μm.

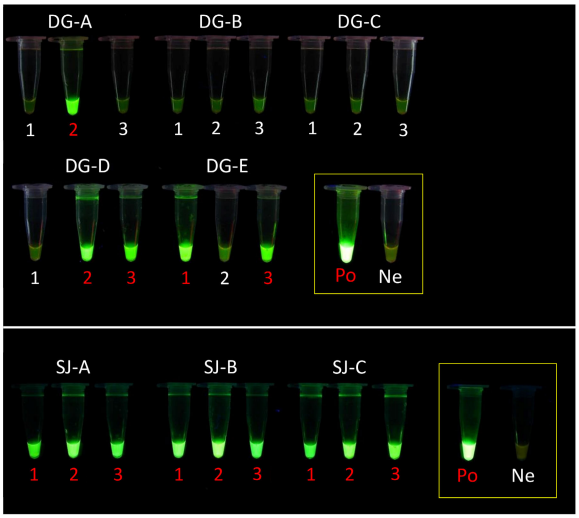

FIGURE 7. Representative LAMP experiment results from each orchard. Examination: 160511 (Mid of May). DG: Daegu orchard, SJ: Sangju orchard, Po: positive control (*M. coronaria* template DNA), Ne: Negative control, white color numbers emphasize healthy samples and red color numbers emphasize infected samples.

Fig. 6 illustrates the overall depth dependent normalized total intensity fluctuation of OCT images. The analysis was based on the representative 2D-OCT images acquired on each experimental day. The intensity representation reveals that the overall total OCT intensity exhibits a gradual reduction along with the incubation period. Since the morphological layers are disappeared and vacuum gaps are formed, backscattered intensity is proportionally reduced with the disease progression. Therefore, a gradual reduction of the overall depth dependent normalized total intensity can be confirmed as shown in Fig. 6.

The samples, which were inspected using OCT, underwent on LAMP experiments. After performing a LAMP reaction and then irradiating the UV, bright fluorescence was identified through the infected specimens. Fig. 7 shows the representative results of UV irradiation of the LAMP reaction performed for the specimens collected from each orchard in mid-May. According to the data representation, 5 specimens among 15 total specimens of Daegu orchard were found to be infected, whereas all 9 specimens of Sangju orchard were infected. The LAMP results reveal that Sangju orchard has a high infection rate compared to Daegu orchard, which is corresponded to the annual reports.

To confirm the precision of the developed compact backpack-type OCT system and the proposed experimental protocol, the infection tendency of both orchards was evaluated and compared using OCT and LAMP results as illustrated in Fig. 8. The graphs exhibit the infection rate fluctuation analyzed using both OCT and LAMP experiment results of each plantation during the entire experiment. Although there are slight differences in the infection rate, both OCT and LAMP experimental results clearly show a corresponding tendency to agree with each other. Most importantly, it was

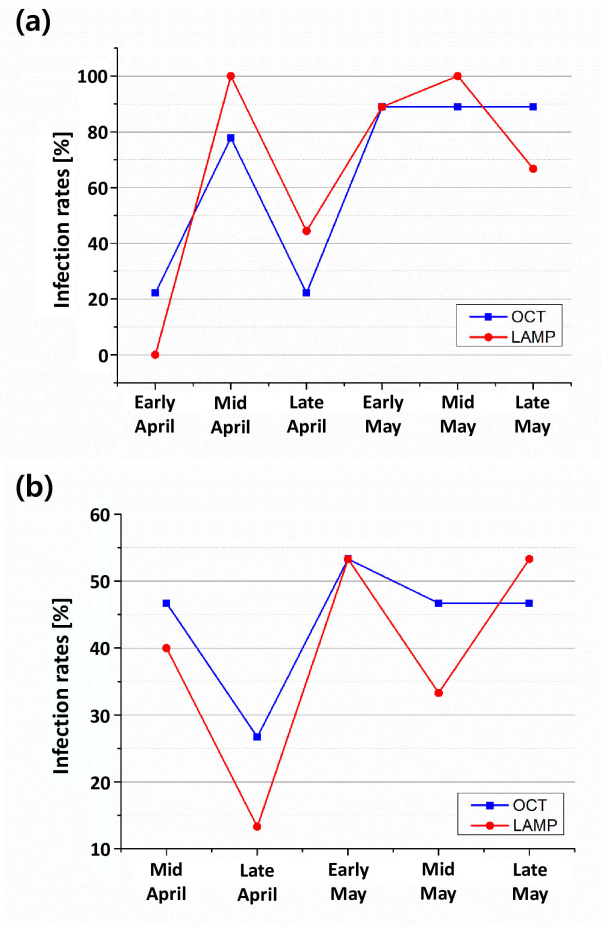

FIGURE 8. OCT and LAMP experiments results comparison by the graph of the infection rates on each experimental days from (a) Sangju plantation and (b) Daegu plantation. OCT and LAMP results is plotted with blue and red line, respectively.

confirmed that the result of the two different methodologies were well correlated with each other, and the tendency was strongly matched before mid-May. Moreover, the results exploit the potential applicability of compact backpack-type OCT system during the period of mid-April to mid-May for the pre-identification of apple blotch, while providing alerts to use specific fungicides for *M. coronaria*. According to the productive related research studies reported during past two decades, scattering of apple blotch conidia starts in early April [36, 37]. Since, the primary infection period is occurred at an early stage of the year, utilization of non-destructive compact backpack-type OCT system during afore stated period to pre-identify the primary infection can be a beneficial fact to control apple blotch at a prior stage. Since the infection rate depends on differences of orchard temperature, humidity, and utility of insect pesticides on each experimental day, these particular external factors can be considered as fundamental reasons for the mismatch between infection ratios. However, the correlation between OCT and LAMP results is sufficiently observed, confirming on-field *in situ* inspection capability of the customized compact backpack-type OCT system.

The non-destructive inspection capability of compact backpack-type OCT was well exploited for apple blotch infected leaf structural properties with a precise real-time agricultural confirmation obtained through LAMP method, which has not been studied descriptively. Although the movements of the OCT system lead to slight resolution contractions, the usefulness of the developed hybrid inspection protocol was confirmed through the visualizations of internal vacuum gap formations. Additionally, an automated image analysis procedure was succeeded in identifying structural abnormalities based on leaf layer intensity information, while directly providing guidance to the identification of apparent infections. Based on these promising findings, the main conceptual and experimental objective of the study was focused towards the potential successful applicability of compact backpack-type OCT for the advance inspection of apple blotch disease.

IV. CONCLUSION

In conclusion, on-field *in situ* inspection procedure for apple blotch using compact backpack-type OCT and LAMP technique is demonstrated. The proposed hybrid inspection protocol was conducted by using laboratory customized fully compact backpack-type OCT system and a well-known agricultural plant disease inspection technique called LAMP. The immediate on-field classified results of the inspection protocol exhibited a successful correlation between OCT and LAMP visualizations confirming the direct applicability of OCT for on-field agricultural inspections. Moreover, the necessity of previously performed time consuming histological evaluations were completely minimized through the demonstrated hybrid inspection due to the rapid readings of both OCT and LAMP techniques. The further advancements of the developed compact backpack-type OCT system can be an ideal pragmatic solution for the inspection of diverse specimens in agricultural plantations, which is helpful to overcome the drawbacks that occur during laboratory-based experiments. Therefore, the developed hybrid inspection protocol using compact backpack-type OCT and LAMP technique can be exploited as a valuable detection process for various agricultural researches.

ACKNOWLEDGMENT

(Junsoo Lee, Seung-Yeol Lee, and Ruchire Eranga Wijesinghe contributed equally to this work.)

REFERENCES

[1] D.-H. Lee, C.-G. Back, N. K. K. Win, K.-H. Choi, K.-M. Kim, I.-K. Kang, C. Choi, T.-M. Yoon, J. Y. Uhm, and H.-Y. Jung, "Biological characterization of *Marssonina coronaria* associated with apple blotch disease," *Mycobiology*, vol. 39, pp. 200–205, Sep. 2011.

[2] C.-G. Back and H.-Y. Jung, "Biological characterization of *Marssonina coronaria* infecting apple trees in Korea.," *Korean J. Mycol.*, vol. 42, no. 3, pp. 183–190, 2014.

[3] G. Tamietti and A. Matta, "First report of leaf blotch caused by *Marssonina coronaria* on apple in Italy.," *Plant Disease*, vol. 87, p. 1005, Aug. 2003.

[4] R. K. Saiki, S. Scharf, F. Faloona, K. B. Mullis, G. T. Horn, H. A. Erlich, and N. Arnheim, "Enzymatic amplification of beta-globin genomic sequences and restriction site analysis for diagnosis of sickle cell anemia," *Science*, vol. 230, pp. 1350–1354, Dec. 1985.
[5] R. K. Saiki, D. H. Gelfand, S. Stoffel, S. J. Scharf, R. Higuchi, G. T. Horn, K. B. Mullis, and H. A. Erlich, "Primer-directed enzymatic amplification of DNA with a thermostable DNA polymerase," *Science*, vol. 239, pp. 487–491, Jan. 1988.
[6] S. Abramowitz, "Towards inexpensive DNA diagnostics," *Trends Biotechnol.*, vol. 14, pp. 397–401, Oct. 1996.
[7] T. Iwamoto, T. Sonobe, and K. Hayashi, "Loop-mediated isothermal amplification for direct detection of *Mycobacterium tuberculosis* complex, M. Avium, and M. Intracellulare in sputum samples," *J. Clin. Microbiol.*, vol. 41, no. 6, pp. 2616–2622, 2003.
[8] Y. Mori and T. Notomi, "Loop-mediated isothermal amplification (LAMP): A rapid, accurate, and cost-effective diagnostic method for infectious diseases," *J. Infection Chemotherapy*, vol. 15, pp. 62–69, Apr. 2009.
[9] T. Notomi, H. Okayama, H. Masubuchi, T. Yonekawa, K. Watanabe, N. Amino, and T. Hase, "Loop-mediated isothermal amplification of DNA," *Nucleic Acids Res.*, vol. 28, p. e63, Jun. 2000.
[10] J. P. Dukes, D. P. King, and S. Alexandersen, "Novel reverse transcription loop-mediated isothermal amplification for rapid detection of foot-and-mouth disease virus," *Arch. Virol.*, vol. 151, pp. 1093–1106, Jun. 2006.
[11] M. A. Shahin, E. W. Tollner, R. W. McClendon, and H. R. Arabnia, "Apple classification based on surface bruises using image processing and neural networks," *Trans. ASAE*, vol. 45, pp. 1619–1627, Sep./Oct. 2002.
[12] J. J. Gonzalez, R. C. Valle, S. Bobroff, W. V. Biasi, E. J. Mitcham, and M. J. McCarthy, "Detection and monitoring of internal browning development in 'Fuji' apples using MRI," *Postharvest Biol. Technol.*, vol. 22, pp. 179–188, May 2001.
[13] R. M. L. McKay, G. R. Palmer, X. P. Ma, D. B. Layzell, and B. T. A. McKee, "The use of positron emission tomography for studies of long-distance transport in plants: Uptake and transport of ^{18}F," *Plant, Cell Environ.*, vol. 11, pp. 851–861, Dec. 1988.
[14] D.-W. Sun and B. Li, "Microstructural change of potato tissues frozen by ultrasound-assisted immersion freezing," *J. Food Eng.*, vol. 57, pp. 337–345, May 2003.
[15] M. R. Hee, J. A. Izatt, E. A. Swanson, D. Huang, J. S. Schuman, C. P. Lin, C. A. Puliafito, and J. G. Fujimoto, "Optical coherence tomography of the human retina," *Arch. Ophthalmol.*, vol. 113, no. 3, pp. 325–332, Mar. 1995.
[16] R. E. Wijesinghe, K. Park, P. Kim, J. Oh, S.-W. Kim, K. Kim, B.-M. Kim, M. Jeon, and J. Kim, "Optically deviated focusing method based high-speed SD-OCT for in vivo retinal clinical applications," *Opt. Rev.*, vol. 23, pp. 307–315, Apr. 2016.
[17] D. Fried, J. Xie, S. Shafi, J. D. Featherstone, T. Breunig, and C. Q. Le, "Imaging caries lesions and lesion progression with polarization-sensitive optical coherence tomography," *J. Biomed. Opt.*, vol. 7, pp. 618–628, Jun. 2002.
[18] R. E. Wijesinghe, N. H. Cho, K. Park, M. Jeon, and J. Kim, "Bio-Photonic detection and quantitative evaluation method for the progression of dental caries using optical frequency-domain imaging method," *Sensors*, vol. 16, no. 12, p. 2076, 2016.
[19] A. F. Fercher, "Optical coherence tomography," *J. Biomed. Opt.*, vol. 1, no. 2, pp. 157–173, Apr. 1996.
[20] N. H. Cho, J. H. Jang, W. Jung, and J. Kim, "*In vivo* imaging of middle-ear and inner-ear microstructures of a mouse guided by SD-OCT combined with a surgical microscope," *Opt. Express*, vol. 22, no. 8, pp. 8985–8995, 2014.
[21] J. Welzel, "Optical coherence tomography in dermatology: A review," *Skin Res. Technol.*, vol. 7, no. 1, pp. 1–9, 2001.
[22] P. Verboven, A. Nemeth, M. K. Abera, E. Bongaers, D. Daelemans, P. Estrade, E. Herremans, M. Hertog, W. Saeys, E. Vanstreels, B. Verlinden, M. Leitner, and B. Nicolaï, "Optical coherence tomography visualizes microstructure of apple peel," *Postharvest Biol. Technol.*, vol. 78, pp. 123–132, Apr. 2013.
[23] M. Li, P. Verboven, A. Buchsbaum, D. Cantre, B. Nicolaï, J. Heyes, A. Mowat, and A. East, "Characterising kiwifruit (Actinidia sp.) near skin cellular structures using optical coherence tomography," *Postharvest Biol. Technol.*, vol. 110, pp. 247–256, Dec. 2015.
[24] S.-Y. Lee, C. Lee, J. Kim, and H.-Y. Jung, "Application of optical coherence tomography to detect *Cucumber green mottle mosaic virus* (CGMMV) infected cucumber seed," *Horticulture, Environ., Biotechnol.*, vol. 53, pp. 428–433, Oct. 2012.
[25] C. Lee, S.-Y. Lee, J.-Y. Kim, H.-Y. Jung, and J. Kim, "Optical sensing method for screening disease in melon seeds by using optical coherence tomography," *Sensors*, vol. 11, no. 10, pp. 9467–9477, 2011.
[26] C.-H. Lee, S.-Y. Lee, H.-Y. Jung, and J.-H. Kim, "The application of optical coherence tomography in the diagnosis of Marssonina blotch in apple leaves," *J. Opt. Soc. Korea*, vol. 16, no. 2, pp. 133–140, 2012.
[27] N. K. Ravichandran, R. E. Wijesinghe, M. F. Shirazi, K. Park, S.-Y. Lee, H.-Y. Jung, M. Jeon, and J. Kim, "*In vivo* monitoring on growth and spread of gray leaf spot disease in *Capsicum annuum* leaf using spectral domain optical coherence tomography," *J. Spectrosc.*, vol. 2016, Dec. 2016, Art. no. 1093734.
[28] R. E. Wijesinghe, S.-Y. Lee, N. K. Ravichandran, S. Han, H. Jeong, Y. Han, H.-Y. Jung, P. Kim, M. Jeon, and J. Kim, "Optical coherence tomography-integrated, wearable (backpack-type), compact diagnostic imaging modality for *in situ* leaf quality assessment," *Appl. Opt.*, vol. 56, no. 9, pp. D108–D114, 2017.
[29] R. Wijesinghe, S.-Y. Lee, N. K. Ravichandran, M. F. Shirazi, and P. Kim, "Optical screening of Venturianashicola caused Pyruspyrifolia (Asian pear) scab using optical coherence tomography," *Int. J. Appl. Eng. Res.*, vol. 11, no. 12, pp. 7728–7731, 2016.
[30] I. V. Meglinski, C. Buranachai, and L. A. Terry, "Plant photonics: Application of optical coherence tomography to monitor defects and rots in onion," *Laser Phys. Lett.*, vol. 7, no. 4, p. 307, 2010.
[31] V. V. Sapozhnikova, V. A. Kamenskii, and R. V. Kuranov, "Visualization of plant tissues by optical coherence tomography," *Russian J. Plant Physiol.*, vol. 50, pp. 282–286, Mar. 2003.
[32] T. H. Chow, K.-M. E. Tan, B.-K. Ng, R. S. Gulam, C. M. Tay, T. F. Chia, and W. T. Poh, "Diagnosis of virus infection in orchid plants with high-resolution optical coherence tomography," *J. Biomed. Opt.*, vol. 14, no. 1, 2009, Art. no. 014006.
[33] M. Jeon, J. Kim, U. Jung, C. Lee, W. Jung, and S. A. Boppart, "Full-range k-domain linearization in spectral-domain optical coherence tomography," *Appl. Opt.*, vol. 50, no. 8, pp. 1158–1163, 2011.
[34] S. Han, O. Kwon, R. E. Wijesinghe, P. Kim, U. Jung, J. Song, C. Lee, M. Jeon, and J. Kim, "Numerical-sampling-functionalized real-time index regulation for direct k-domain calibration in spectral domain optical coherence tomography," *Electron.*, vol. 7, p. 182, 2018.
[35] F. Catté, P.-L. Lions, J.-M. Morel, and T. Coll, "Image selective smoothing and edge detection by nonlinear diffusion," *SIAM J. Numer. Anal.*, vol. 29, no. 1, pp. 182–193, 1992.
[36] D.-A. Kim, S.-W. Lee, and J.-T. Lee, "Ecology of Marssonina blotch caused by Diplocarpon mali on apple tree in Kyungpook, Korea," *Current Res. Agricult. Life Sci.*, vol. 16, pp. 84–95, Dec. 1998.
[37] J. Y. Uhm, *Reduced Fungicide Spray Program for Major Apple Diseases Korea*. Korea: Culture and Horticulture Press, 2010.

JUNSOO LEE received the B.E. degree in electronics engineering from Kyungpook National University, Daegu, South Korea, in 2018, where he is currently a M.D. Researcher with the Electronics Engineering Department. His research interests include development of optical system for medical application, photoacoustic tomography, and development and applications for spectral domain optical coherence tomography.

SEUNG-YEOL LEE received the Ph.D. degree in applied biosciences from Kyungpook National University, Daegu, South Korea, where he has been an Assistant Professor with the School of Applied Biosciences, since 2018. His research interests include diagnosis of fruit diseases, molecular phylogenetic analysis of plant pathogens, and development of fungal isolation method.

RUCHIRE ERANGA WIJESINGHE received the B.Sc. and Ph.D. degrees in electronics engineering from Kyungpook National University, Daegu, South Korea, in 2012 and 2018, respectively. He is currently an Assistant Professor with the Department of Biomedical Engineering, Kyungil University. His research interests include development of high-resolution novel biological and biomedical imaging techniques, including optical coherence tomography and microscopy for clinical utility.

NARESH KUMAR RAVICHANDRAN received the B.E. degree in electronics and communication engineering from St. Peter's University, Chennai, India, and the M.Sc. degree in electronics engineering from Kyungpook National University, Daegu, South Korea, where he has been a Ph.D. Researcher with the Electronics Engineering Department, since 2016. His research interests include developing and optimizing novel biological imaging techniques with possible applications in dental, agronomical studies, entomological studies, and industrial applications.

SANGYEOB HAN is currently pursuing the Ph.D. degree with the School of Electronics Engineering, Kyungpook National University, Daegu, South Korea. His research interests include optical imaging techniques, photoacoustic microscopy, optical coherence tomography, and multiphoton microscopy.

PILUN KIM received the Ph.D. degree from the Department of Medical and Biological Engineering, Kyoungpook National University, in 2011, where he is currently a Researching Visiting Professor with the Institute of Biomedical Engineering. He is interested in translating new technologies from the research field to the application field, such as clinic and industrial and making its productization. His main research interests include biomedical device development, optical coherence tomography, and digital image processing.

MANSIK JEON received the Ph.D. degree in electronics engineering from Kyungpook National University, Daegu, South Korea, in 2011, where he is currently an Assistant Professor with the School of Electronics Engineering. His research interests include development of nonionizing and noninvasive novel biomedical imaging techniques, including photoacoustic tomography, photoacoustic microscopy, optical coherence tomography, ultrasonic imaging, handheld scanner, and their clinical applications.

HEE-YOUNG JUNG received the Ph.D. degree in applied biosciences from the University of Tokyo, Japan. He is currently a Professor with the School of Applied Biosciences, Kyungpook National University. His research interests include control of fruit tree diseases, development of plant disease diagnosis method, mushroom cultivation, microbial systematics, and various plant disease.

JEEHYUN KIM received the Ph.D. degree in biomedical engineering from the University of Texas at Austin, USA, in 2004. He was a Postdoctoral Researcher with the Beckman Laser Institute, University of California at Irvine. He is currently a Professor with Kyungpook National University, Daegu, South Korea. His research interests include biomedical imaging and sensing, neuroscience studies using multiphoton microscopy, photoacoustic imaging, and other novel applications of sensors.